Standing Alfvén Waves in the Magnetosphere

W. D. CUMMINGS AND R. J. O'SULLIVAN

Department of Planetary and Space Science
University of California, Los Angeles, California 90024

P. J. COLEMAN, JR.

Department of Planetary and Space Science and
Institute of Geophysics and Planetary Physics
University of California, Los Angeles, California 90024

Transverse, low-frequency oscillations in the magnetic field have been recorded in the equatorial plane at 6.6 R_E (earth radii) with the UCLA magnetometer on board ATS 1. The oscillations have peak-to-peak amplitudes of 2 to 20 γ and have been observed predominantly on geomagnetically quiet days in the morning and noon quadrants. The fluctuations are very nearly monochromatic, and those with periods ranging from 50 to 300 sec have been studied. This paper reports on observations made during January 1967, when 25 separate events were recorded with durations ranging from 10 to 400 min. The oscillations could be grouped into two period ranges, one centered about $T = 190$ sec and the other about $T = 102$ sec. The oscillations were confined to a plane that was approximately perpendicular to the main magnetic field vector. They were generally elliptically polarized in this plane, with the major axis of the polarization ellipse typically inclined eastward at an angle of $\simeq 30°$ to the radially outward direction. An MHD analysis is given for an idealized model in which the earth is considered a perfect conductor, the background magnetic field is that of a dipole, and the plasma density varies as a power law. For the case of a standing Alfvén wave the poloidal and toroidal wave equations uncouple. These equations are solved numerically, and the eigenfrequencies appropriate to the synchronous orbit are tabulated for the first six harmonics for seven density models. From the results of the analysis it is argued that the observed transverse oscillations are the second harmonic of a standing Alfvén wave. Under this interpretation the data are consistent with the hypothesis that the plasmapause is beyond 6.6 R_E only during very quiet periods.

INTRODUCTION

Several types of fluctuations observed in the distant geomagnetic field have been interpreted in terms of hydromagnetic waves [cf. *Coleman et al.*, 1960; *Sonett et al.*, 1962; *Judge and Coleman*, 1962; *Nishida and Cahill*, 1964; *Patel and Cahill*, 1964; *Patel*, 1965, 1966]. In all of these cases, the satellite was apparently in motion at rather high velocities relative to the plasma in which the waves were propagating at the time of their observation. The recorded oscillations seldom included more than a few cycles, and in most cases they could be described at best as quasi-sinusoidal.

We report here on low-frequency, nearly monochromatic oscillations of the geomagnetic field that have been detected on magnetically quiet days at the synchronous, equatorial orbit of ATS 1. (Transverse oscillations similar to those reported here have also been detected by magnetometers on board the DODGE satellite as a geocentric distance of 6.2 R_E (A. J. Zmuda, personal communication).) This geostationary satellite is located at 150°W longitude, so that it is close to the intersection of the geomagnetic and geographic equatorial planes. The orbit is nearly circular with a mean radius of 6.6 R_E (1 R_E = radius of the earth). The geographic latitude of the spacecraft was held at $0° \pm 0.5°$ during the period of observation reported here. ATS 1 is spin-stabilized, with a spin rate of $\simeq 1.6$ revolutions per second. The ATS 1 magnetometer is a biaxial, fluxgate magnetometer. Because of the rotation of the vehicle, the magnetometer can be used to measure the vector field in the absence of field fluctuations with

frequencies above about half the rotation frequency. The magnetometer experiment has been described briefly by *Cummings and Coleman* [1968] and in more detail by *Barry and Snare* [1966].

Observations

The vector magnetic field will be described in terms of its components in a coordinate system rotating with the earth, the *DHV* system (see Figure 1). In this system, D and V are the components of the field in the geographic equatorial plane; D is positive eastward, and V is positive outward. The H direction is positive northward, i.e., perpendicular to the geographic equatorial plane and parallel to the earth's spin vector.

During magnetically quiet days sinusoidal fluctuations in the magnetic field at ATS 1 are often observed for intervals up to several hours. The fluctuations are generally amplitude-modulated. Measurements taken during a typical

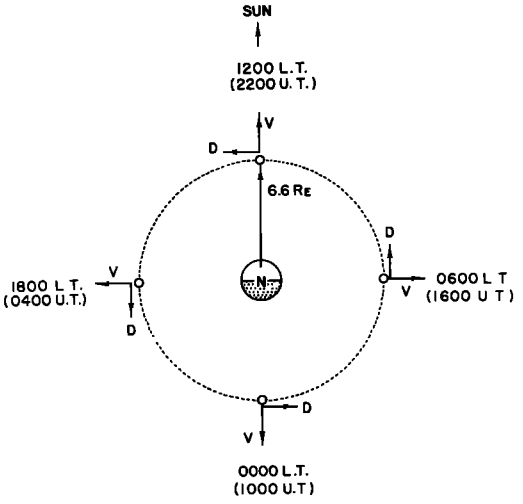

Fig. 1. The *DHV* coordinate system has its origin at the satellite and corotates with it at 150°W longitude in the geographic equatorial plane. D is positive eastward, V is positive outward, and H is positive northward, i.e., perpendicular to the equatorial plane.

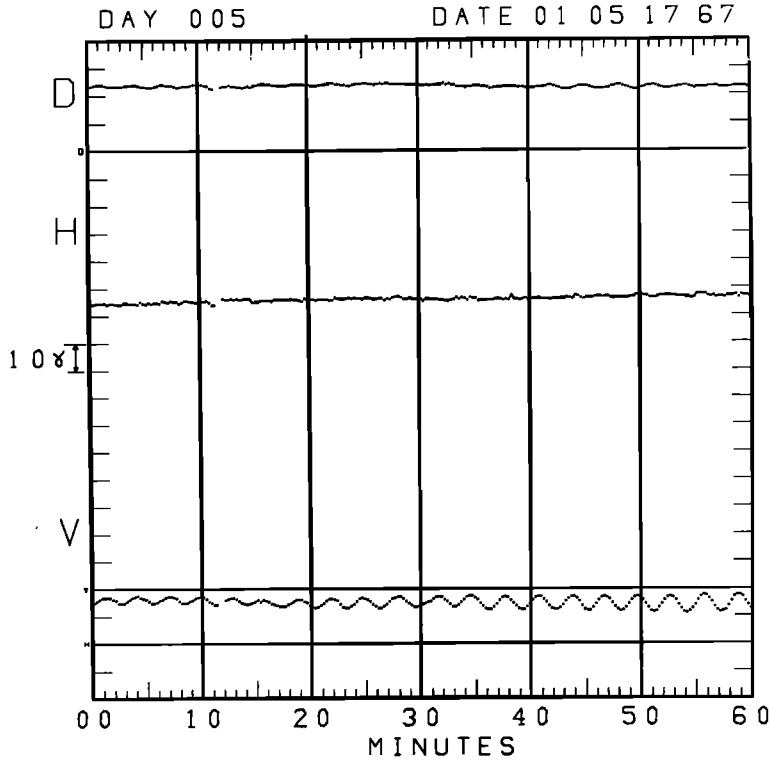

Fig. 2. An example of the transverse oscillations observed at ATS 1. The magnetogram covers one hour; each point is a 15-sec average of the data. The starting time (UT) for the hour is given in the upper right-hand corner (month, day, hour, year). The three horizontal lines denote zero levels for the three components of the field.

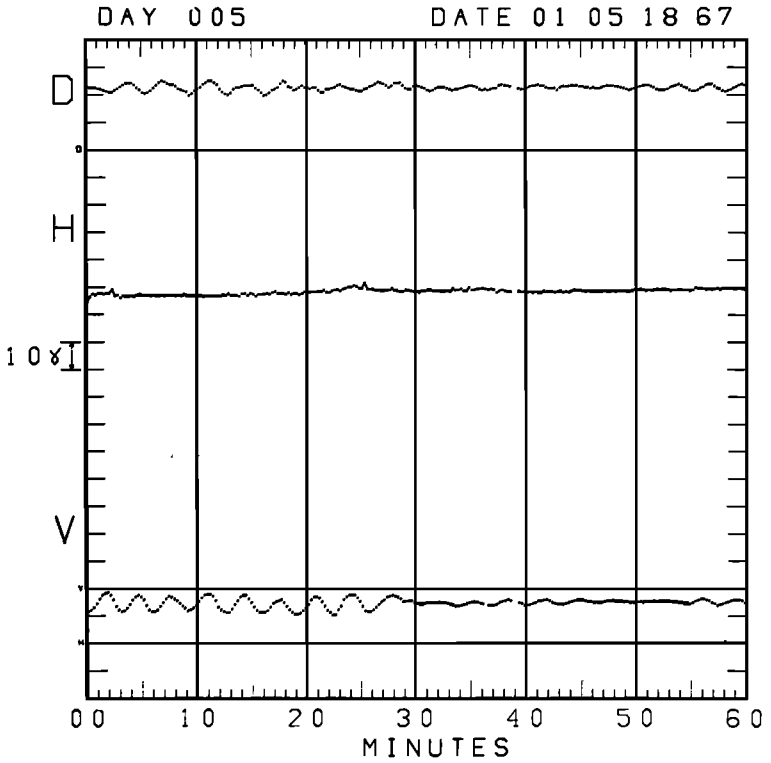

Fig. 3. Continuation of Figure 2.

event are plotted in Figures 2–4 (hours 1700–1900 UT, January 5, 1967). The data points are 15-second averages.

We will consider here fluctuations with periods ranging approximately 50 sec to approximately 300 sec. Within this range, lower-frequency fluctuations generally have larger amplitudes. Amplitudes between 1 and 10 γ have been recorded. During the event shown in Figures 2–4, the field variations had amplitudes of less than 10 γ peak-to-peak and a period of about 180 sec.

For the purposes of this initial report, a simple method was used to determine the period of the oscillations during each 10-min interval in which they were detected. An integral number of cycles was selected so that the total time interval, τ

$$\tau = \sum_{i=1}^{n} T_i$$

where T_i equals the period of the ith cycle, corresponded as closely as possible to the given 10-min interval. The average period for the 10-min interval was then determined as $T = \tau/n$. Only data for which $Kp < 3-$ were used in determining the period in this way.

Figure 5 is a plot of the period T as a function of local time for the oscillations that were detected during the month of January 1967. The oscillations occurred mainly during the daylight hours, and there is a strong morning-evening asymmetry in the occurrence distribution. Note the absence of oscillations in the dusk-midnight sector. In the month of January 1967, there were 3190 ten-minute intervals for which $Kp < 3-$ and for which ATS 1 data were available. During 146 of these intervals, or 4.6% of the total, there were fluctuations with waveforms clear enough to permit the use of the procedure for determining the period. For the 3-hour interval 1900–2100 UT (0900–1200 LT) oscillations could be observed 7.8% of the time that Kp was $<3-$. Usually, whenever the sinusoidal oscillations were not occurring, there were no field fluctuations with amplitudes greater than 1 γ in the frequency range studied here.

We have found that for a given event the

period of the oscillations remains essentially constant. In this respect, Figure 5 is perhaps misleading since each data point represents a measurement of the period over a 10-min interval rather than the measure of the period for the entire event. We have therefore included Table 1, which lists the duration, average period, and the maximum amplitude of the D and V components of all the events observed in January 1967.

As can be seen from the histogram on the right-hand side of Figure 5, the oscillations could be grouped into two period ranges, $T > 2.5$ and $T < 2.5$. The average period for the first group was $T_1 = 3.17 \pm 0.35$ min (190 ± 21 sec) and for the second group $T_2 = 1.71 \pm 0.33$ min (102 ± 20 sec), where the quoted errors represent one standard deviation. Figures 2–4 show an example of the oscillations from the first group. For these oscillations, $T \simeq 180$ sec. An example of oscillations from the second group is shown in Figure 6. In this case, $T \simeq 90$ sec.

A correlation between the period and Kp was found. In Figure 5, we have indexed each point by the value of Kp for the 3-hour interval in which the oscillation occurred. Note that the oscillations in the range $T > 2.5$ min occurred mainly when $Kp < 1$.

In general, the perturbation vectors of the January 1967 oscillations were rather well confined to a plane during each event. The oscillations were elliptically polarized. Sometimes the ellipticity was extremely high, i.e., the polarization was nearly linear. For several events it was possible to determine the angle between the mean magnetic field vector and the plane containing the oscillations. The orientation of the plane was determined by using the principal-axis technique. In this method, the normal coordinates are obtained by diagonalizing the variance tensor

$$S_{ij} = (1/n) \sum_{\mu=1}^{n} [B_i^{\mu} - \langle B_i^{\mu} \rangle][B_j^{\mu} - \langle B_j^{\mu} \rangle]$$

where B_i^{μ} is the ith component of the μth field measurement, and

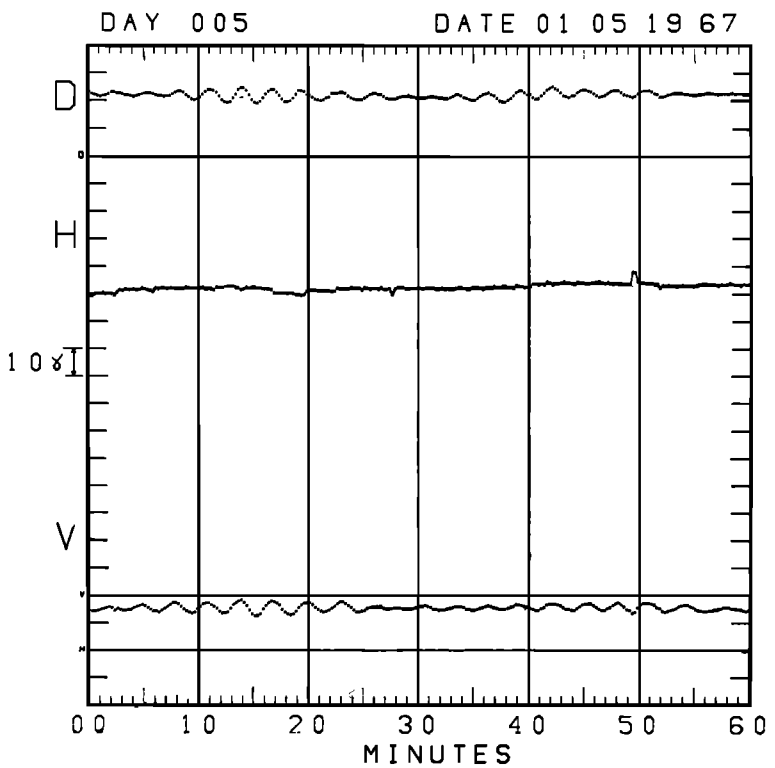

Fig. 4. Continuation of Figure 3.

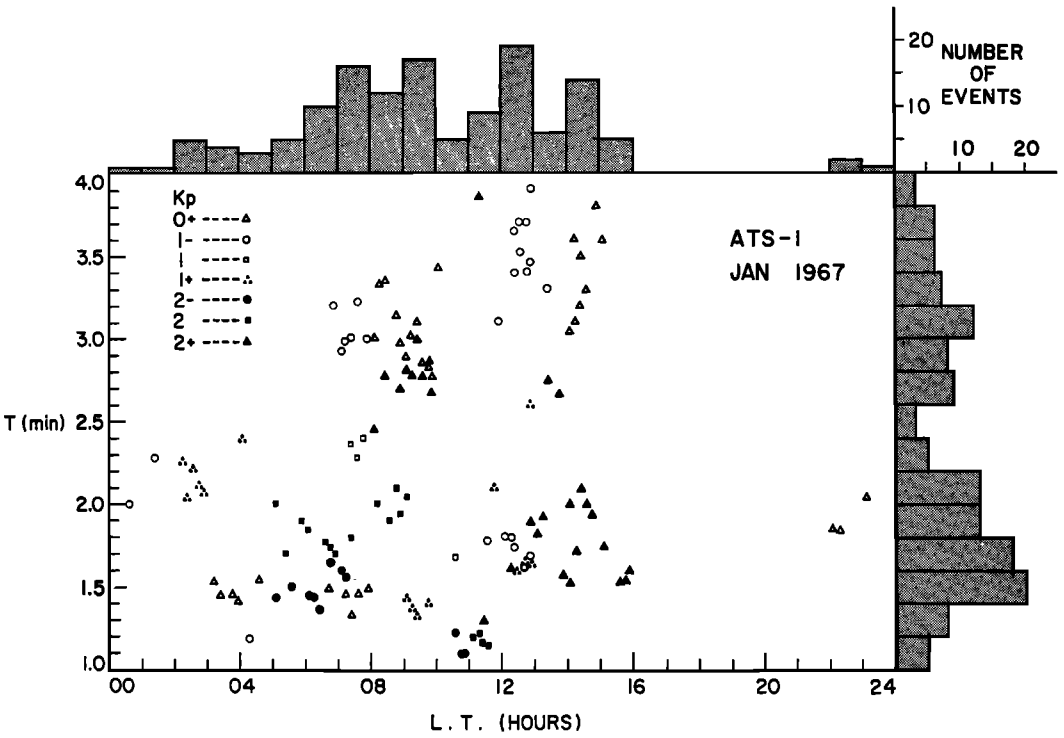

Fig. 5. Each measurement of the wave period over a 10-minute interval is plotted as a function of local time. A different symbol is used for each of 7 values of the geomagnetic activity index, K_p, in the range 0+ to 2+. The histogram at the top of the figure indicates a local-time dependence that is very similar to that given by *Sucksdorff* [1939] (see his Figure 4). The histogram at right indicates that the oscillations occur in two period ranges centered about $T_1 \simeq 3.2$ min and $T_2 \simeq 1.7$ min. The oscillations with higher periods tend to occur only during very quiet conditions ($K_p < 1+$).

$$\langle B_i^{\mu} \rangle = (1/n) \sum_{i=1}^{n} B_i^{\mu}$$

The normal coordinates are then the principal axes of the variance ellipsoid in the transformed coordinate system.

When the oscillations are confined to a plane, the normal to the plane is the unit vector associated with the least variance. For oscillations confined purely to a plane, one of the three variances will be zero. For linearly polarized oscillations, two of the variances will be zero, and the normal coordinate associated with the third variance will be in the direction of the oscillations.

In practice, for the linearly polarized oscillations observed at ATS 1 two of the variances were much smaller than the third. The angle between the mean field and the normal coordinate associated with the largest variance was usually very nearly 90°. For example, this angle varied between 83.3° and 94.7° for the oscillations shown in Figures 2–4.

In most cases, the variance ellipsoid is really an ellipse, the plane of which is perpendicular to the mean magnetic field vector. The orientation of the major axis of this ellipse is of interest. Since the mean field is essentially along H, it is sufficient to determine the orientation of the projection of the ellipse on the DV plane. The distribution of the angle Ψ between the V direction and the major axis of the ellipse, as projected on the DV plane, is shown in Figure 7.

We can summarize the observed properties of these low-frequency oscillations at the synchronous orbit as follows:

1. The oscillations were detected almost exclusively in the local-time range 0200–1500.

2. The periods were grouped into two ranges, one centered about $T = 190$ sec, the other about $T = 102$ sec.

3. The oscillations with $T \simeq 190$ were usually observed during very quiet (geomagnetically) conditions.

4. The oscillations were confined to a plane that was approximately perpendicular to the mean magnetic field.

5. The oscillations were elliptically polarized in this plane. The preferred angle from the V direction to the major axis of the ellipse was approximately 30°.

Analysis

Several ground-based observations of sinusoidal oscillations in the magnetic field have been reported. The most striking examples in the frequency range of interest are the geomagnetic giant pulsations, Pg [*Rolf,* 1931; *Harang,* 1932; *Sucksdorff,* 1939]. These unique sinusoidal oscillations are observed simultaneously in conjugate areas near the auroral zones [*Sugiura,* 1961; *Nagata et al.,* 1963; *Annexstad and Wilson,* 1968]. They occur predominantly in the morning hours and, in fact, *Sucksdorff* [1939] reported a local-time distribution that is similar to our Figure 5. The oscillations have amplitudes in the range $\simeq$1–100 γ and periods of $\simeq$100 seconds. The giant pulsations may last for as long as a few hours. As observed on the surface of the earth, coherent vibrations are considerably localized [*Rolf,* 1931; *Veldkamp,* 1960; *Annexstad and Wilson,* 1968].

It has been suggested that the Pg's are caused by field-line guided hydromagnetic waves [*Obayashi and Jacobs,* 1958; *Veldkamp,* 1960; *Annexstad and Wilson,* 1968]. Several authors have attributed the magnetic pulsations to hydromagnetic wave resonances within the magnetosphere, deriving the eigenperiods from a travel-time equation [e.g., *Obayashi and Jacobs,* 1958; *MacDonald,* 1961].

Others have considered primarily only the

TABLE 1. Transverse Oscillations Observed at ATS 1, January 1967

Event Number	Universal Time: Beginning d h m	Universal Time: Ending d h m	Duration, min	Average Period, min	Maximum Peak to Peak D, γ	Maximum Peak to Peak V, γ
1	1 23 50	2 00 16	26	1.6	4	6
2	2 22 30	2 23 00	30	1.6	3	4
3	4 16 40	4 18 00	80	1.4	2	3
4	4 20 30	4 20 40	10	1.7	1	2
5	5 11 10	5 11 60	50	2.3	1	2
6	5 16 50	6 00 30	460	3.2	6	9
7	6 21 35	6 21 47	12	1.8	4	8
8	6 22 00	6 23 00	60	1.7	4	4
9	8 21 10	8 21 20	10	3.9	6	9
10	8 21 20	8 21 34	14	1.3	5	10
11	8 22 10	9 02 00	230	1.9	15	20
12	9 20 10	9 21 38	88	1.2	5	6
13	10 13 10	10 17 20	250	1.6	3	4
14	18 08 00	18 08 20	20	1.9	4	3
15	18 10 00	18 10 50	50	2.0	1	3
16	18 12 10	18 13 20	70	2.1	2	5
17	18 13 50	18 14 10	20	2.4	1	3
18	18 15 00	18 19 30	270	1.9	5	6
19	18 21 00	18 22 10	70	2.1	6	9
20	19 17 10	19 20 00	170	2.7	6	6
21	19 22 10	19 23 20	70	2.6	4	5
22	22 18 00	22 20 00	120	1.4	2	4
23	29 23 50	30 02 00	130	3.6	5	5
24	31 08 50	31 09 10	20	2.1	2	4
25	31 22 10	31 23 00	50	3.7	2	4

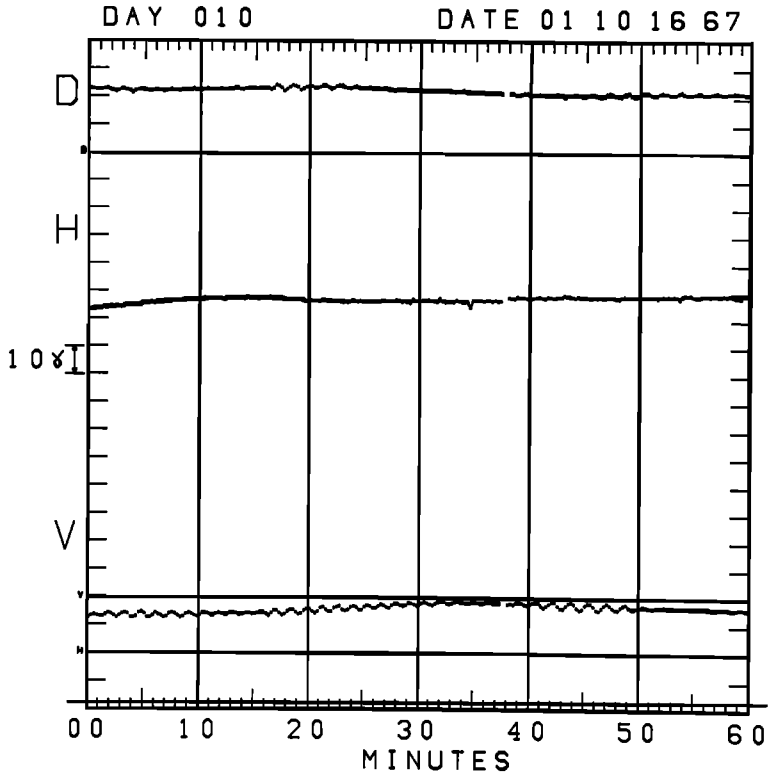

Fig. 6. An example of transverse oscillations with period in the second range, $T \simeq 1.5$ min.

axisymmetric modes of oscillation [e.g., *Dungey,* 1963; *Radoski and Carovillano,* 1966]. The analysis given here is essentially an extension of that given by *Radoski* [1967*a, b*]; it is not restricted to either the axisymmetric toroidal modes or the highly asymmetric poloidal modes.

Before describing our analysis, we will review the previous measurements concerning the magnetospheric plasma in the vicinity of the synchronous orbit.

1. A field-aligned density discontinuity (the plasmapause) separates a region (the plasmasphere) in which the equatorial electron concentration is $\simeq$100/cm^3 from a region (the plasmatrough) in which the equatorial density is $\simeq$1/cm^3 [*Carpenter,* 1963, 1966].

2. In the local-time range 0000–1800 the geocentric equatorial distance to the plasmapause is usually less than 4 R_E for moderately disturbed days, i.e., Kp = 2–4 [*Carpenter,* 1966]. However, for magnetically quiet conditions the equatorial distance to the plasmapause is sometimes beyond the synchronous orbit [*Carpenter,* 1966; *Taylor et al.,* 1968].

3. In the plasmatrough the density decreases approximately as r^{-4}. In the plasmasphere the density distribution along the field lines is in approximate agreement with a diffusive equilibrium model, which gives a much less rapid decrease than the r^{-4} in the model [*Angerami and Carpenter,* 1966].

Since the observed wave frequencies ($\simeq$0.01 Hz) are much lower than the lowest characteristic frequency, the proton cyclotron frequency ($\simeq$2 Hz), an analysis that uses MHD equations and assumes a cold, collisionless background plasma is probably justified. Such an analysis is given below and is rigorously applicable only to the following idealized model of the earth and its magnetosphere:

1. The earth is a perfect conductor.
2. The earth has an external dipole magnetic field.
3. The background plasma is cold and collisionless.
4. The plasma density varies as r^{-m}, where m is an adjustable positive parameter.

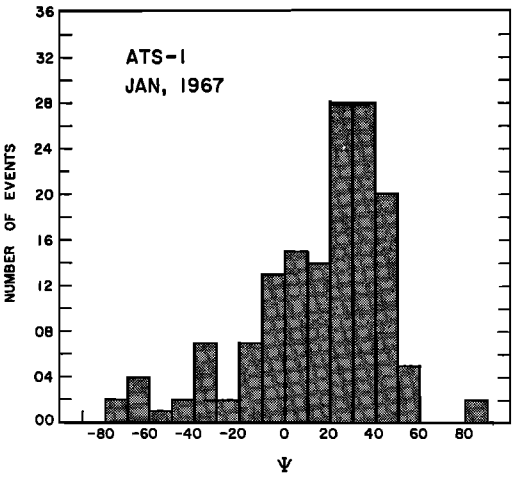

Fig. 7. Histogram showing the number of events, i.e., 10-min intervals, as a function of the angle Ψ between the V direction and the major axis of the polarization ellipse. Positive angles are measured from V toward positive D.

In addition to these assumptions about the medium, we make two assumptions about any possible mode of oscillation, namely:

5. All wave quantities have a time dependence of the form $e^{i\omega t}$.

6. The components of the wave electric and magnetic field parallel to the background magnetic field line are zero.

The last assumption insures that the Poynting vector for the wave is always parallel to the background magnetic field lines. The propagation is therefore analogous to that in a transmission line (TEM mode), rather than that in a waveguide (TE or TM mode). The TM waveguide mode can probably be ruled out because the electric field in a collisionless plasma must be transverse to the field lines. The TE mode is unlikely because the transverse dimension of the 'guide' is much smaller than a wavelength for these very low frequencies. For a more complete discussion of these points, see *Booker* [1962], *Cummings and Dessler* [1967], and *Fejer and Lee* [1968].

The resonance oscillation can best be described in terms of the orthogonal dipole coordinate system. The unit vectors for this system are illustrated in Figure 8 for various positions on the ATS 1 field line. The unit vector $\mathbf{e}_\mu$ is parallel to the field line, $\mathbf{e}_\nu$ is in the direction of the principal normal to the field line, and $\mathbf{e}_\phi$ is in the azimuthal direction. The coordinates are: $\nu = (\sin^2\theta)/r$, which is constant along a dipole field line; $\mu = (\cos\theta)/r^2$, which is constant along an orthogonal trajectory of the dipole field lines; and ϕ, which is the ordinary azimuthal spherical polar coordinate.

The linearized wave equation for low-frequency propagation in a cold, collisionless, magnetized plasma is

$$\partial^2\mathbf{E}/\partial t^2 = \mathbf{A} \times \mathbf{A} \times \text{curl curl } \mathbf{E} \qquad (1)$$

where $\mathbf{E}$ is the electric field of the wave, $\mathbf{A} = \mathbf{B}/(\mu_0\rho)^{1/2}$ = the Alfvén velocity, and $\mathbf{B}$ = the background magnetic field (mks units are used except where otherwise specified). If one assumes a time dependence of the form $e^{i\omega t}$ and that the electric field parallel to the background magnetic field is zero, equation 1 takes the component form

$$H_1[\partial/\partial\mu(H_2\partial\epsilon_\nu/\partial\mu) + \partial/\partial\phi(\partial\epsilon_\nu/\partial\phi - \partial\epsilon_\phi/\partial\nu)] + (\omega^2/A^2)\epsilon_\nu = 0 \qquad (2)$$

$$H_2[\partial/\partial\mu(H_1\partial\epsilon_\phi/\partial\mu) - \partial/\partial\nu(\partial\epsilon_\nu/\partial\phi - \partial\epsilon_\phi/\partial\nu)] + (\omega^2/A^2)\epsilon_\phi = 0 \qquad (3)$$

where

$$H_1 = (\nu r^3)^{-1}$$
$$H_2 = \nu(1 + 3\cos^2\theta)r^{-3}$$
$$\epsilon_\nu = r^2E_\nu/[(1 + 3\cos^2\theta)^{1/2}\sin\theta]$$

and

$$\epsilon_\phi = r\sin\theta E_\phi$$

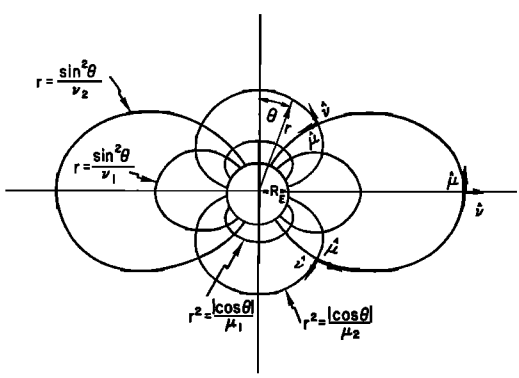

Fig. 8. An illustration of the orthogonal dipole coordinate system. The curves of constant ν are the dipole field lines and the curves of constant μ are the orthogonal trajectories to the field lines. The unit vectors μ and ν are shown for three positions on the ATS 1 field line.

For a guided wave in which the Poynting vector is always along the field line, the magnetic wave field is transverse to the background magnetic field. Hence, the wave field along the field line is

$$B_\mu = (-i/\omega)(\nabla \times \mathbf{E})_\mu \tag{4}$$

or

$$B_\mu = (-i/\omega)[(1 + 3\cos^2\theta)^{1/2}/r^3] \cdot (\partial\epsilon_\phi/\partial\nu - \partial\epsilon_\nu/\partial\phi) = 0$$

When this condition is imposed, equations 2 and 3 are no longer coupled, and we have

$$H_1\,\partial/\partial\mu(H_2\,\partial\epsilon_\nu/\partial\mu) + (\omega^2/A^2)\epsilon_\nu = 0 \tag{5}$$

$$H_2\,\partial/\partial\mu(H_1\,\partial\epsilon_\phi/\partial\mu) + (\omega^2/A^2)\epsilon_\phi = 0 \tag{6}$$

To solve equations 5 and 6 for a given value of ν, i.e., for a given field line, one must adopt a model for the plasma density distribution (in using the orthogonal dipole system we, of course, also assume the earth's field is that of a dipole). In subsequent calculations, we will adopt the model of a hydrogen plasma with a number density distribution that varies as

$$n = n_0(r_0/r)^m$$

where $r_0 = 1/\nu$ = the geocentric distance to the equatorial crossing point of the field line under consideration, and n_0 is the proton number density at r_0. Since $r = r_0 \sin^2\theta$ for a dipole field line, the number density varies along the field line as $n = n_0 \sin^{-2m}\theta$. The background magnetic field varies along the field line as

$$B = B_0(1 + 3\cos^2\theta)^{1/2}/\sin^6\theta$$

where B_0 is the field strength at the equatorial crossing point of the field line. Therefore, in this model, the square of the Alfvén speed varies along the field line as

$$A^2 = B_0^2(1+3\cos^2\theta)/[\mu_0 m_p n_0(1-\cos^2\theta)^{6-m}]$$

where m_p denotes the proton mass.

With these substitutions, equations 5 and 6 can be rewritten as

$$\partial^2\epsilon_\nu/\partial z^2 + kC(1-z^2)^{6-m}\epsilon_\nu = 0 \tag{7}$$

$$\partial^2\epsilon_\phi/\partial z^2 - 6z/(1+3z^2)\partial\epsilon_\phi/\partial z + CK(1-z^2)^{6-m}\epsilon_\phi = 0 \tag{8}$$

where $z = \cos\theta$; $C = (r_0/R_E)^6 r_0^2\mu_0 m_p/B_E^2$; B_E = the surface field strength at the earth's equator, taken to be 3.12×10^{-5} w/m^2; $k = \omega^2 n_0$ = the eigenvalue for the toroidal equation 5; and $K = \omega^2 n_0$ = the eigenvalue for the poloidal equation 6.

Note that since equations 7 and 8 are entirely independent we have allowed for the possibility that the eigenvalues are different. If the eigenvalues are different, the analysis here is, in general, not valid since assumption 5 is violated. From equation 4 we see that B_μ could not be independent of time and, in general, would not be zero. We will refer to these points again in the Interpretations section.

We have numerically solved equations 7 and 8 by using the boundary condition that $\epsilon_\nu = \epsilon_\phi = 0$ at $z = \pm z_0 = \pm(1 - R_E/r_0)^{1/2}$, i.e., at the surface of the earth. The eigenvalues k_i and K_i determined by these boundary conditions are listed in Table 2 for the first six harmonics. For the tabulated results the equatorial number density is 1/cm^3. The eigenperiod for any other number density can be obtained from Table 2 by using the relation $T = T_0(n)^{1/2}$, where T_0 is the period given in the table and n is the desired number density in units of cm^{-3}.

The magnetic wave vector is related to the electric wave vector by Faraday's law

$$\nabla \times \mathbf{E} = -\partial\mathbf{B}/\partial t$$

For a resonance oscillation with a time dependence of the form $e^{i\omega t}$, Faraday's law yields

$$B_\nu = \frac{i}{\omega}\frac{(1+3\cos^2\theta)^{1/2}}{r^4\sin\theta}\frac{\partial\epsilon_\phi}{\partial\mu} = \frac{i}{\omega}\frac{1}{r_0^2(1+3z^2)^{1/2}(1-z^2)^{3/2}}\frac{\partial\epsilon_\phi}{\partial z} \tag{9}$$

$$B_\phi = -\frac{i}{\omega}\frac{(1+3\cos^2\theta)}{r^5}\sin\theta\frac{\partial\epsilon_\nu}{\partial\mu} = -\frac{i}{\omega}\frac{1}{r_0^3(1-z^2)^{3/2}}\frac{\partial\epsilon_\nu}{\partial z} \tag{10}$$

Once ϵ_ϕ and ϵ_ν are numerically determined as functions of z, it is possible to determine B_ν and B_ϕ from equations 9 and 10. From equation 9 we see that the amplitude of B_ν is proportional to $(1/\omega) \times$ amplitude of E_ϕ, and from equation 10, the amplitude of B_ϕ is proportional to $(1/\omega) \times$ amplitude of E_ν. The amplitudes B_ϕ and E_ν are plotted as functions of θ in Figure

TABLE 2. Theoretical Eigenperiods and Eigenfrequencies of the Uncoupled Toroidal and Poloidal Wave Equations

A density distribution of the form $n = n_0(6.6\ R_E/r)^m$ has been assumed, and n_0 was taken as $1/cm^3$ for these calculations.

Density Index, m	Harmonic Index, h	(1 cm^{-3} density) Period, sec		(1 cm^{-3} density) Frequency, Hz	
		Toroidal	Poloidal	Toroidal	Poloidal
	1	52.2	71.9	.019	.014
	2	19.8	20.1	.051	.050
0	3	12.2	12.3	.082	.082
	4	8.9	8.9	.113	.113
	5	7.0	6.9	.144	.144
	6	5.7	5.7	.175	.175
	1	53.5	73.6	.019	.014
	2	20.9	21.2	.048	.047
1	3	13.0	13.0	.077	.077
	4	9.4	9.4	.106	.106
	5	7.4	7.4	.135	.135
	6	6.1	6.1	.164	.164
	1	54.9	75.6	.018	.013
	2	22.2	22.5	.045	.045
2	3	13.9	14.0	.072	.072
	4	10.1	10.1	.099	.099
	5	8.0	8.0	.125	.125
	6	6.6	6.6	.152	.152
	1	56.7	77.9	.018	.013
	2	23.8	24.1	.042	.042
3	3	15.1	15.1	.066	.066
	4	11.0	11.0	.091	.091
	5	8.7	8.7	.115	.115
	6	7.2	7.2	.139	.139
	1	58.9	80.6	.017	.012
	2	25.9	26.1	.039	.038
4	3	16.6	16.6	.060	.060
	4	12.2	12.2	.082	.082
	5	9.7	9.7	.103	.103
	6	8.0	8.0	.125	.125
	1	61.6	84.0	.016	.012
	2	28.7	28.8	.035	.035
5	3	18.7	18.8	.054	.053
	4	13.9	13.9	.072	.072
	5	11.0	11.0	.091	.091
	6	9.2	9.2	.109	.109
	1	65.3	88.5	.015	.011
	2	32.7	32.7	.031	.031
6	3	21.8	21.9	.046	.046
	4	16.3	16.4	.061	.061
	5	13.1	13.1	.077	.076
	6	10.9	10.9	.092	.092

9. A similar plot of B_r and E_ϕ would be identical to Figure 9, except for slight differences in the fundamental mode. In Figure 9 we have used a plasma distribution of the form $n = n_0 (r_0/r)^3$, i.e., for $m = 3$. However, only very minor changes in the waveforms occur for values of m in the range 0–6. To demonstrate this, we have plotted in Figure 10 the second-harmonic amplitudes of B_ϕ and E_r for $m = 0$, 3, and 6. Plots of B_r and E_ϕ are also presented in Figure 10 to illustrate their similarity with the plots of B_ϕ and E_r.

In Figures 9 and 10 we have normalized the wave magnetic field to the value that would be

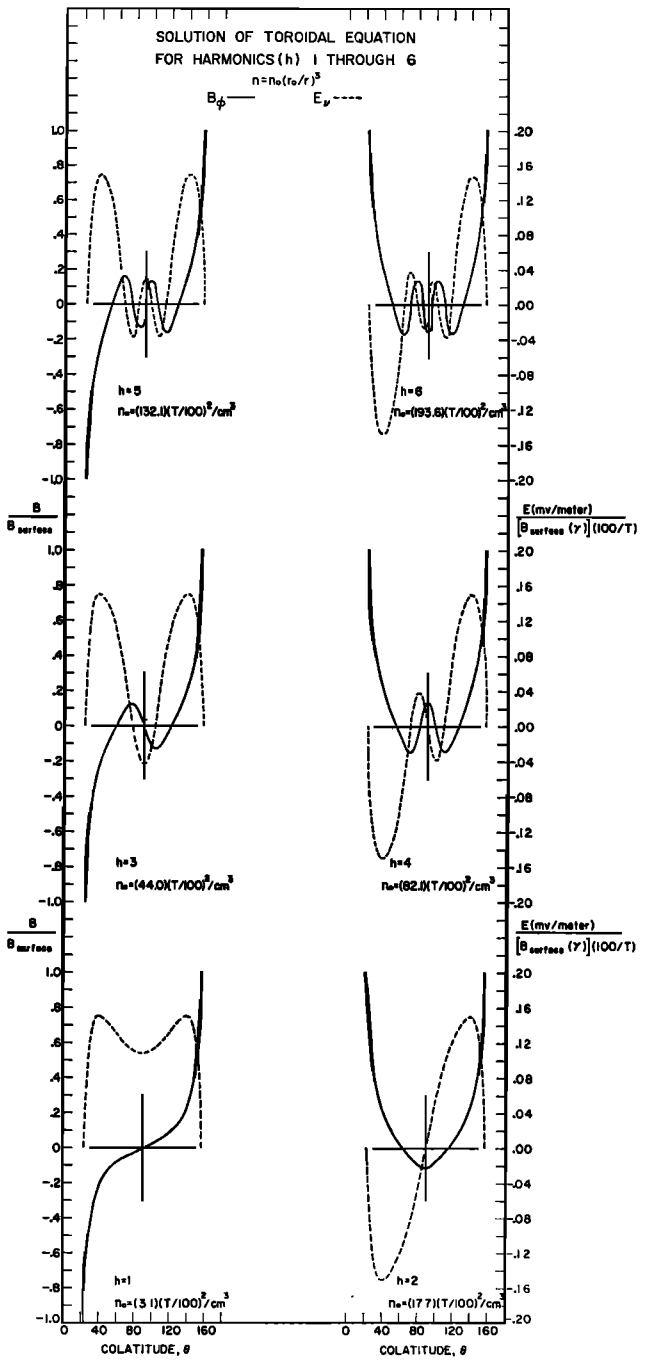

Fig. 9. Solutions of the toroidal equation for $m = 3$. The theoretical wave magnetic field at any point along the field line can be obtained from the left ordinate by multiplying by the surface field value. Similarly, the wave electric field amplitude can be obtained from the right ordinate by multiplying by the indicated factors. The equation beneath each figure gives the equatorial number density as a function of period.

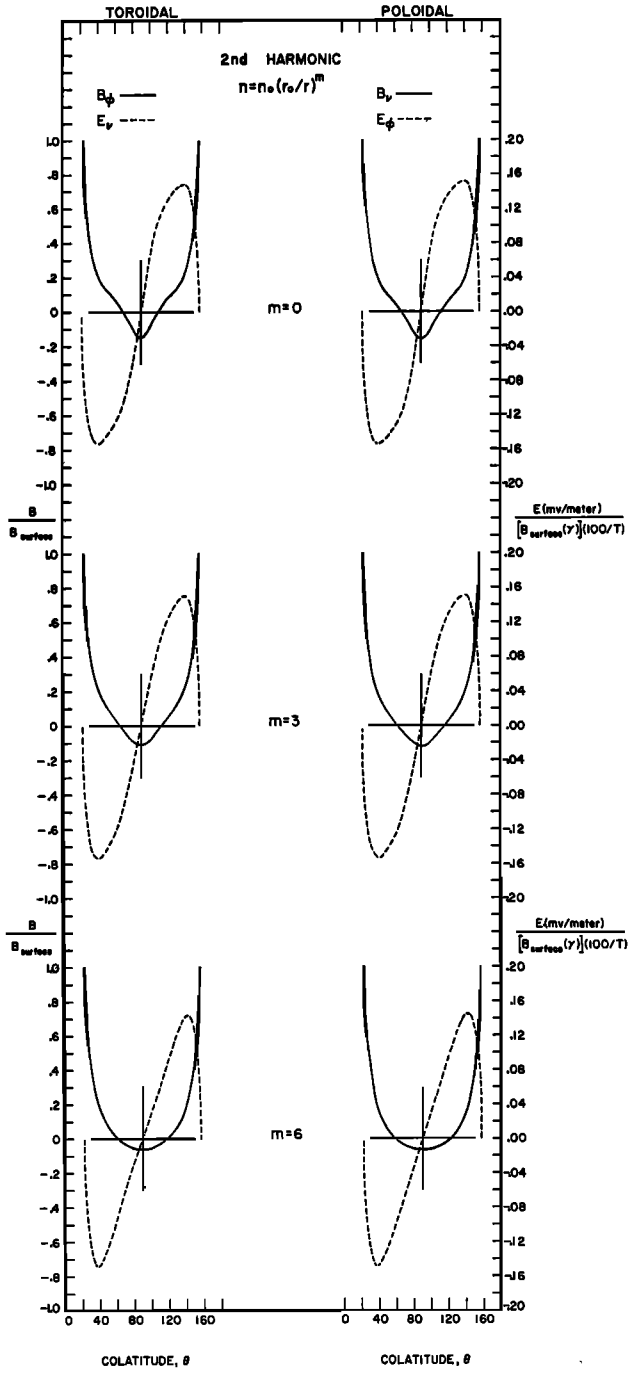

Fig. 10. The second harmonic solutions of the toroidal and poloidal wave equations for density indices $m = 0$, 3, and 6. The wave magnetic and electric fields at any point along the ATS 1 field line can be obtained by the same procedure as described in Figure 9.

observed at the reflecting surface of the perfect conductor [$B_{surface}(\gamma)$]. The amplitude of the wave magnetic field at any point along the field can be determined by multiplying the left-hand ordinate by $B_{surface}(\gamma)$. The amplitude of the wave electric field at any point along the field line can be determined from this graph by multiplying the right-hand ordinate by $B_{surface}(\gamma)$ divided by the wave period expressed in hundreds of seconds. The equatorial number density determined from the eigenvalue for each harmonic can be evaluated from the equation given beneath each set of curves. For example, suppose an oscillation is observed in the auroral zone with 10-γ amplitude and 100-sec period. If the oscillation represents the second harmonic of the standing wave resonance, then the magnetic wave amplitude near the synchronous orbit should be $\simeq 1$ γ, and the peak electric field wave amplitude should be $\simeq 1.5$ mv/m and should occur along the field line at $\theta \simeq 40°$ and 140°.

Interpretations

From Table 2 we see that the poloidal and toroidal eigenfrequencies for the fundamental mode are significantly different. Thus assumption (5) is violated, and, as previously noted, our analysis is generally invalid for this mode. We interpret this result to mean that the fundamental mode at the standing Alfvén wave cannot occur at ATS 1 except in the special case when $\epsilon_\phi = 0$ and $\partial\epsilon_\mu/\partial\phi = 0$, which is the case of a toroidal oscillation of field shells [*Dungey*, 1963; *Radoski and Carovillano*, 1966].

If ATS 1 were sufficiently distant from the geomagnetic equatorial plane, one might expect to see evidence of this axisymmetric oscillation. The variations would be in B_ϕ, i.e., in the D component of the field. However, the oscillations that are observed often occur in both D and V. Further, as Figures 2–4 illustrate, the oscillations are sometimes primarily in V. We thus conclude that the oscillations observed at ATS 1 do not represent the fundamental mode of the MHD standing wave resonance.

The poloidal and toroidal eigenfrequencies are approximately equal for all harmonics above the fundamental. The observations at ATS 1 are probably of the even harmonics, since the magnetic wave amplitude is zero at the equatorial plane for the odd harmonics. Assuming the background field is that of a dipole, ATS 1 was within 2.2° of the geomagnetic equatorial plane throughout January 1967.

We have prepared Table 3 to facilitate a comparison between the ATS 1 observations and the results of the analysis. In the table we have listed the predicted equatorial number densities for the various assumed plasma distributions. The average periods $T_1 = 190$ sec and $T_2 = 102$ sec were used in calculating the average number densities listed in the table. On either side of the average number densities are the number densities corresponding to $T \pm \delta T$, where δT is one standard deviation about the average periods discussed in the Observations section.

The lowest densities listed (6.3–13.9/cm^3) correspond to $m = 6$ for the second harmonic and are associated with oscillations in the second period range, i.e., $T \simeq T_2$. These number densities are somewhat higher than the 1–5/cm^3 previously reported for the plasmatrough [*Carpenter*, 1963, 1966; *Taylor et al.*, 1968].

Densities of $\simeq 100$/cm^3, corresponding to the plasmasphere, can be obtained from various combinations of assumed plasma distributions and harmonic levels. Perhaps the most plausible assumption is that both oscillations with $T \simeq T_1$ and those with $T \simeq T_2$ represent the 2nd harmonic of the standing wave resonance. For oscillations with $T \simeq T_1$, number densities of the order of 100/cm^3 can be obtained from a plasma distribution that is independent of geocentric distance, i.e., $m = 0$.

The above results are in good qualitative, and fair quantitative, agreement with previous measurements of the background plasma distribution. However, before the standing wave interpretation can be considered satisfactory, a number of other points must be examined.

Firstly, the theory predicts that the magnetic wave amplitude observed at the reflecting surface will be a factor of 10 larger than the magnetic wave amplitude in the equatorial plane. The oscillations reported by *Sucksdorff* [1939] at Sodankyla, Finland (geomagnetic latitude 63.8°), rarely had amplitudes greater than 10 γ. Those reported by *Annexstad and Wilson* [1968] at College (geomagnetic latitude 64.6°) and Macquarie Island (geomagnetic latitude −61.1°) had perhaps somewhat higher amplitudes, but they rarely exceeded 30 γ. Although we do not yet have a simultaneous satellite-earth surface

TABLE 3. Computed Equatorial Proton Number Density (cm^{-3}) for All Density Indices m, $0 \leqq m \leqq 6$ and Harmonic Levels h, $2 \leqq h \leqq 6$

The two average periods $T_1 = 190$ sec and $T_2 = 102$ sec were used for these computations. Also included in the table are computed number densities for $T_1 \pm \delta T_1$, and $T_2 \pm \delta T_2$, where δT_1 and δT_2 represent one standard deviation about the average values (see text).

Harmonic Index, h	Density Index, m	Density No., cm^{-3}					
		$T_1 - 21$ 169	T_1 190	$T_1 + 21$ 211	$T_2 - 20$ 82	T_2 102	$T_2 + 20$ 122
	0	70.7	89.4	110.3	16.7	25.8	36.9
	1	63.6	80.4	99.2	15.0	23.2	33.2
	2	57.3	72.4	89.3	13.5	20.9	29.9
2	3	49.9	63.0	77.7	11.7	18.2	26.0
	4	42.3	53.5	65.9	10.0	15.4	22.0
	5	34.4	43.5	53.6	8.1	12.5	17.9
	6	26.8	33.8	41.7	6.3	9.8	13.9
	0	189.9	240.0	296.0	44.7	69.2	99.0
	1	168.4	212.9	262.5	39.6	61.3	87.8
	2	147.1	185.9	229.3	34.6	53.6	76.6
3	3	125.4	158.5	195.4	29.5	45.7	65.3
	4	103.5	130.8	161.3	24.4	37.7	53.9
	5	81.2	102.7	126.6	19.1	29.6	42.3
	6	59.9	75.7	93.3	14.1	21.8	31.2
	0	363.6	459.6	566.8	85.6	132.4	189.5
	1	320.5	405.1	499.6	75.5	116.7	167.0
	2	277.3	350.5	432.2	65.3	101.0	144.5
4	3	234.5	296.4	365.5	55.2	85.4	122.2
	4	191.2	241.6	298.0	45.0	69.6	99.6
	5	148.1	187.2	230.9	34.9	54.0	77.2
	6	106.8	135.0	166.4	25.1	38.9	55.6
	0	592.1	748.4	923.0	139.4	215.7	308.6
	1	520.3	657.6	811.0	122.5	189.5	271.1
	2	448.4	566.7	698.9	105.6	163.3	233.4
5	3	377.3	476.9	588.1	88.8	137.4	196.6
	4	305.1	385.7	475.6	71.8	111.1	159.0
	5	234.6	296.5	365.7	55.2	85.5	122.3
	6	116.8	210.8	259.9	39.3	60.7	86.9
	0	875.0	1105.9	1363.9	206.0	318.7	456.0
	1	767.2	969.7	1195.9	180.6	279.5	399.8
	2	660.4	834.7	1029.4	155.6	240.6	344.1
6	3	553.0	698.9	862.0	130.2	201.4	288.2
	4	445.7	563.4	694.8	104.9	162.4	232.3
	5	341.1	431.1	531.6	80.3	124.2	177.7
	6	240.7	304.3	375.2	56.7	87.7	125.4

measurement of the wave amplitudes, it appears that the ratio $B_{\text{surface}}/B_{\text{equatorial plane}}$ is somewhat lower than predicted. The ratio would be lower than predicted by our analysis if the effective reflecting surface is below the earth's surface, which is certainly the case.

Secondly, to account for the long wavetrains observed at ATS 1, we must assume that either the energy loss of the earth-magnetosphere system is extremely small or some source, perhaps broadband, is feeding energy to the resonant mode, or both. Wave energy can be lost by failure of exact guidance along the field line by Joule dissipation at the reflection surface, i.e., inside the earth, or by Joule dissipation in the ionosphere where the wave changes its character from hydromagnetic to electromagnetic.

Thirdly, the eigenvalues obtained from our analysis are actually functions of ϕ and ν, i.e., they apply to a single field line and not to the magnetosphere as a whole. *Radoski* [1967] has raised this point in objecting to the concept of oscillating field lines. The observation by *Annexstad and Wilson* [1968] and others that the Pg

pulsations seem to occur only near the auroral zone suggests that it is unnecessary to assume extensive coupling between field lines so that all oscillate at the same frequency. If the main point of energy loss is in the ionosphere, then a standing wave might only occur along field lines that pass through the ionosphere in a region of high conductivity, i.e., the auroral zone. The oscillations would then be expected to occur only on field lines having L values within a narrow range, so that all the lines in this range would have approximately the same eigenfrequency.

Ionospheric filtering, i.e., resonances in the micropulsation transmission coefficient [cf. *Prince and Bostick*, 1964; *Greifinger and Greifinger*, 1965; *Field and Greifinger*, 1965], could also lead to the occurrence of oscillations only within a narrow L range. In this case, oscillations might only occur on L shells having eigenfrequencies corresponding to the resonant frequencies for the ionospheric transmission coefficient.

Despite the above reservations, which have not been examined in detail, there is reasonable agreement between theory and experiment if we interpret the oscillations observed at ATS 1 as the second harmonic of an MHD standing wave resonance. According to this interpretation, the oscillations with $T \simeq T_1$ represent the standing wave when the plasmapause is beyond the geosynchronous orbit. In agreement with previous observations: (1) the number density in the plasmasphere is $\simeq 100/\text{cm}^3$; (2) the distribution of plasma along the field line is roughly independent of geocentric distance; and (3) the equatorial geocentric distance to the plasmapause is greater than 6.6 R_E only for very quiet geomagnetic conditions. The oscillations with $T \simeq T_2$ must represent the standing wave when the plasmapause is inside the geosynchronous orbit. The predicted equatorial number density is $\simeq 10/\text{cm}^3$, somewhat higher than previously observed. However, in agreement with previous observations, we find that the density along the field line in the plasmatrough must decrease extremely rapidly with geocentric distance.

There is one other significant point of agreement between conjugate point observations and our interpretation of the oscillations as the second harmonic of the standing wave resonance. Note from Figures 9 and 10 that, for the second harmonic, B_ϕ at one end of the field line is in phase with B_ϕ at the other end of the field line. Similarly, B_r is in phase at the conjugate points of a field line. At the earth's surface, in both northern and southern hemispheres, B_ϕ corresponds approximately to D. However, as can be seen from Figure 8, B_r corresponds to $+H$ in the northern hemisphere and $-H$ in the southern hemisphere. Therefore, for the second harmonic, D should be in phase and H should be out of phase at the conjugate points. These are precisely the observations reported for Pg micropulsations observed simultaneously at conjugate stations. In fact, on the basis of arguments by analogy with the elastic string model of magnetic field lines, other authors have similarly concluded that the Pg micropulsations must represent an even (i.e., $m = 2, 4, \ldots$) mode of oscillation [*Sugiura and Wilson*, 1964].

Acknowledgments. The authors have benefited from helpful discussions with Drs. J. M. Cornwall, A. J. Dessler, J. W. Dungey, J. A. Fejer, C. F. Kennel, R. L. McPherron, H. R. Radoski, and W. B. Thompson.

This research was supported in part by the National Aeronautics and Space Administration under contract NAS 5-9570.

References

Angerami, J. J., and D. L. Carpenter, Whistler studies of the plasmapause in the magnetosphere, 2, Electron density and total tube electron content near the knee in magnetospheric ionization, *J. Geophys. Res.*, *71*, 711, 1966.

Annexstad, J. O., and C. R. Wilson, Characteristics of Pg micropulsations at conjugate points, *J. Geophys. Res.*, *73*, 1805, 1968.

Barry, J. D., and R. C. Snare, A fluxgate magnetometer for the Applications Technology Satellite, *IEEE Trans. Nucl. Sci.*, *NS-13*, 326, 1966.

Booker, H. G., Guidance of radio and hydromagnetic waves in the magnetosphere, *J. Geophys. Res.*, *67*, 4135, 1962.

Carpenter, D. L., Whistler evidence of a 'knee' in the magnetospheric ionization density profile, *J. Geophys. Res.*, *68*, 1675, 1963.

Carpenter, D. L., Whistler studies of the plasmapause in the magnetosphere, 1, Temporal variations in the position of the knee and some evidence on plasma motions near the knee, *J. Geophys. Res.*, *71*, 693, 1966.

Coleman, P. J., Jr., C. P. Sonett, D. L. Judge, and E. J. Smith, Some preliminary results of the Pioneer 5 magnetometer experiments, *J. Geophys. Res.*, *65*, 1856, 1960.

Cummings, W. D., and P. J. Coleman, Jr., Simultaneous magnetic field variations at the earth's surface and at synchronous, equatorial distance, 1, Bay-associated events, *Radio Sci.*, *3*, 758, 1968.

Cummings, W. D., and A. J. Dessler, Field-aligned currents in the magnetosphere, *J. Geophys. Res., 72,* 1007, 1967.

Dungey, J. W., in *Geophysics the Earth's Environment,* edited by C. DeWitt, J. Hieblot, and A. Lebeau, p. 537, Gordon and Breach, Science Publishers, New York, 1963.

Fejer, J. A., and K. F. Lee, Guided propagation of Alfvén waves in the magnetosphere, *J. Plasma Phys., 1,* 387, 1967.

Field, E. C., and C. Greifinger, Transmission of geomagnetic micropulsations through the ionosphere and lower exosphere, *J. Geophys. Res., 70,* 4885, 1965.

Greifinger, C., and P. Greifinger, Transmission of micropulsations through the lower ionosphere, *J. Geophys. Res., 70,* 2217, 1965.

Harang, L., Observations of micropulsations in the magnetic records at Tromso, *Terrest. Magnetism Atmospheric Elec., 37,* 57, 1932.

Judge, D. L., and P. J. Coleman, Jr., Observations of low-frequency hydromagnetic waves in the distant geomagnetic field: Explorer 6, *J. Geophys. Res., 67,* 5071, 1962.

MacDonald, G. J. F., Spectrum of hydromagnetic waves in the exosphere, *J. Geophys. Res., 66,* 3639, 1961.

Nagata, T., S. Kokubun, and T. Iijima, Geomagnetically conjugate relationships of giant pulsations at Syowa Base, Antarctica, and Reykjavik, Iceland, *J. Geophys. Res., 68,* 4621, 1963.

Nishida, A., and L. J. Cahill, Jr., Sudden impulses in the magnetosphere observed by Explorer 12, *J. Geophys. Res., 69,* 2243, 1964.

Obayashi, T., and J. A. Jacobs, Geomagnetic pulsations and the earth's outer atmosphere, *Geophys. J., 1,* 53, 1958.

Patel, V. L., Low frequency hydromagnetic waves in the magnetosphere: Explorer 12, *Planetary Space Sci., 13,* 485, 1965.

Patel, V. L., A note on the propagation of hydromagnetic waves in the magnetosphere, *Earth Planetary Sci. Letters, 1,* 282, 1966.

Patel, V. L., and L. J. Cahill, Jr., Evidence of hydromagnetic waves in the earth's magnetosphere and of their propagation to the earth's surface, *Phys. Rev. Letters, 12,* 213, 1964.

Prince, C. E., Jr., and F. X. Bostick, Jr., Ionospheric transmission of transversely propagated plane waves at micropulsation frequencies and theoretical power spectrums, *J. Geophys. Res., 69,* 3213, 1964.

Radoski, H. R., A note on oscillating field lines, *J. Geophys. Res., 72,* 418, 1967*a*.

Radoski, H. R., Highly asymmetric MHD resonances: The guided poloidal mode, *J. Geophys. Res., 72,* 4026, 1967*b*.

Radoski, H. R., and R. L. Carovillano, Axisymmetric plasmasphere resonances: Toroidal mode, *Phys. Fluids, 9,* 285, 1966.

Rolf, B., Giant micropulsations at Abisko, *Terrest. Magnetism Atmospheric Elec., 36,* 9, 1931.

Sonett, C. P., A. R. Sims, and I. J. Abrams, The distant geomagnetic field, 1, Infinitesimal hydromagnetic waves, *J. Geophys. Res., 67,* 1191, 1962.

Sucksdorff, E., Giant pulsations recorded at Sodankyla during 1931–1938, *Terrest. Magnetism Atmospheric Elec., 44,* 157, 1939.

Sugiura, M., Evidence of low-frequency hydromagnetic waves in the exosphere, *J. Geophys. Res., 66,* 4087, 1961.

Sugiura, M., and C. R. Wilson, Oscillation of the geomagnetic field lines and associated magnetic perturbations at conjugate points, *J. Geophys. Res., 69,* 1211, 1964.

Taylor, H. A., Jr., H. C. Brinton, and M. W. Pharo, III, Contraction of the plasmasphere during geomagnetically disturbed periods, *J. Geophys. Res., 73,* 961, 1968.

Veldkamp, J., A giant geomagnetic pulsation, *J. Atmospheric Terrest. Phys., 17,* 320, 1960.

(Received August 30, 1968;
presentation revised October 11, 1968.)